K. Weiser

Properties of GaAs Diodes with P-P^0-N Structures*

Abstract: The electrical and electroluminescent properties of GaAs diodes with P-P^0-N structure are discussed with special emphasis on their negative resistance characteristics. A description is given of the fabrication of diodes, consisting of a central, manganese-doped, high-resistivity layer (the P^0 region) between low-resistivity P- and N-layers. The theory of Dumke for the origin of the negative resistance characteristics is shown to give a good account of their static characteristics. Extension of the theory to transient characteristics (i.e., response to voltage pulses in excess of the breakdown voltage) predicts faster switching speeds than have been observed experimentally; nevertheless, diodes fabricated by one technique switch within a few nanoseconds at room temperature with overvoltages of only a few volts.

List of symbols

P	Low resistivity p-type region
P^0	High resistivity, central p-type region
L	Width of the P^0 region
N	Low resistivity n-type region
V	Voltage across the P^0 region
V_0	Voltage across the P^0 region at the beginning of a voltage pulse
V_{th}	Threshold voltage for the onset of the negative resistance.
V_{th}^I	Threshold voltage for the onset of the negative resistance in the presence of external illumination
V_s	Sustaining voltage of the negative resistance regime
V_t	Voltage at which the transit time of injected electrons equals their lifetime
i	Current
j	Current density
j_{th}	Current density at the onset of the negative resistance regime
p_0	Thermal hole density in the P^0 region
Δn	Electron density created in the P^0 region by light
μ_n	Mobility of electrons
μ_p	Mobility of holes
τ	Lifetime of injected electrons
γ	Quantum efficiency of the recombination process at the P-P^0 boundary
γ_∞	Quantum efficiency of the recombination process at the P-P^0 boundary for currents much higher than j_{th}
b	Current density at which the quantum efficiency reaches one-half its final value
α	Absorption constant for light
ϕ	Fraction of the light emitted at the P-P^0 boundary absorbed in the P^0 region
I	Intensity of external illumination in photons per square centimeter per second
I_{th}	Intensity of external illumination which produces switching when the diodes are biased below V_{th}
t	Time
t_d	Delay time before switching; during this period, current and voltage changes are small
t_s	Switching time during which the voltage decreases and the current increases radically
R	Resistance of load in series with diode
e	Electronic charge
A	Cross-sectional area of the diode in the plane of the junction

* This work was supported by the U. S. Army Signal Supply Agency under Contract (DA 36-039 AMC-02349).

Introduction

The properties of GaAs diodes with a three-layer structure, consisting of a central high resistivity region flanked by low resistivity p- and n-regions, are of considerable interest. Such structures permit the study of the injection of electrons and holes into the high resistivity region and of the recombination of the injected carriers. Since recombination in GaAs is usually radiative it is possible to study its spatial origin as a function of electric field. By varying the nature of the dominant recombination center in the central layer, information about the capture cross section of different centers can be obtained.

Another area of interest for the study of such diodes lies in the field of injection lasers. The fact that each of the three layers has distinctly different optical properties gives rise to well-defined mode guiding effects, and hence to unusual near field and far field patterns of laser light emission.[1a,b,c]

Perhaps the most striking phenomenon exhibited by these diodes is that they generally show a negative resistance over a range of their current-voltage relations and that the critical voltage for its onset is light sensitive. The negative resistance was observed by Holonyak et al.[2a,b] and Ing et al.,[3] using so-called semi-insulating GaAs for the central layer. It was also observed by Yamamoto[4] though in that case it is not clear just why the central region should have been one of high resistivity. It was assumed by these investigators that the phenomenon was the result of a mechanism proposed by Lampert[5] which has its origin in a change of lifetime for injected holes induced by saturation of the dominant recombination centers. Weiser and Levitt[6] found light sensitive, negative resistance behavior in diodes in which the high resistivity of the central region was produced by the presence of manganese. (Chromium may be substituted for manganese as has been demonstrated recently by Pilkuhn and Rupprecht.[1c]) The study of this structure had the advantage that the electrical and electroluminescent properties could be correlated with the known properties of manganese doped GaAs. Weiser and Levitt concluded that the electrical and electroluminescent properties of the diodes before the onset of the negative resistance could be understood satisfactorily on the basis of the theory of Ashley and Milnes[7] for double injection into the central layer. It was concluded, however, that the negative resistance was probably not the result of the mechanism suggested by Lampert. On the other hand, a theory proposed by Dumke[8a,b] appeared to give a good account of the phenomenon observed.

In this paper we wish, first of all, to present Dumke's theory in greater detail than was done in the original publication, giving particular attention to the switching behavior of the diodes. We derive expressions for the negative resistance characteristics using Dumke's model but employ a somewhat different approach which enables us to derive theoretical expressions for the switching time. Since, in previous publications, it has been established that the static electrical and electroluminescent properties of diodes produced by a double diffusion technique[6] are in good agreement with Dumke's model, little space will be devoted in this paper to a re-examination of these properties; we do, however, examine the effect of external illumination on these diodes in greater detail than has been done. We also produce data for diodes prepared by a technique which provides a uniformly doped central region, and show that the static properties are also in satisfactory agreement with the theory. We then compare the prediction of the theory with the switching behavior of both the double diffused diodes and of diodes which contain a uniformly doped central region, and find serious discrepancies between theory and experimental results.

Theory

Nature of the P^0 layer

We shall assume that the high resistivity central region (the P^0 layer or region) is p-type and that its width is many times the diffusion length of either electrons or holes. We shall assume that the field is high enough so that the current is field driven rather than carried by diffusion. The energy level of the dominant impurity should be at least several kT above the valence band and the region should be extrinsic. We shall also require that there be appreciable but not critical compensation present, so that a fraction of all the centers will be negatively charged at all temperatures. We also assume that the compensating donor level is shallow enough so that trapping effects for injected electrons are negligible. In Fig. 1 we show an energy diagram for the model chosen. A central assumption of the model is that the diffusion length of one of the injected carriers is much greater than of the other carrier. The fact that a fraction of the acceptor levels is negatively charged should insure that the capture-cross-section for injected holes is much larger than for injected electrons which would be captured by neutral centers. In the case of GaAs a smaller diffusion length for holes will furthermore be favored by the fact that the mobility of electrons is much greater than that of holes.[9]

Figure 1 Fermi level (E_F) and impurity scheme in P-P^0-N diodes. E_c and E_v are the edges of the conduction and valence bands, respectively. Plus symbols signify ionized donors, minus symbols signify ionized acceptors, and circles correspond to holes. The N- and P-regions are shown as degenerately doped, to agree with the experimental conditions employed.

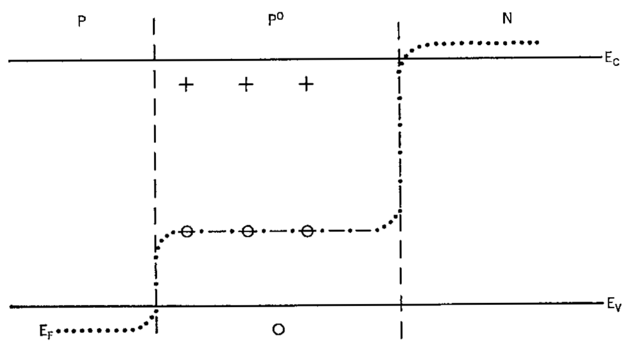

- *Current-voltage relation before the onset of the negative resistance*

The current-voltage relation at small forward bias for the P-P^0-N structure described here was treated theoretically by Ashley and Milnes.[7] Briefly, as the voltage is raised to allow injection of electrons across the P^0-N junction, recombination will at first take place within a diffusion length. For each injected electron a hole will flow across the P^0 layer, and hence the current across it will initially be a hole current. As the applied voltage exceeds the built-in voltage of the junction, a field will develop across the P^0 layer, and the electrons will no longer drift across it by diffusion only. Gradually, therefore, recombination will take place throughout the layer. When the field becomes large enough so that the transit time of electrons becomes less than their lifetime, a majority can traverse the P^0 layer before recombining, and the current will now be carried mainly by electrons. We summarize the current-voltage relation across the P^0 layer, as derived by Ashley and Milnes:

$$j = p_0 e\mu_p V/L, \quad \text{for} \quad V \ll L^2/\mu_n\tau; \tag{1a}$$

$$j = aV^2, \quad \text{for} \quad V \gg L^2/\mu_n\tau \tag{1b}$$

where $a \equiv pe\mu_p\mu_n\tau/L^3$. In these expressions, j is the current density, V the voltage across the P^0 layer (i.e., the total voltage across the diode minus the voltage across the P^0-N junction), p_0 the equilibrium hole density in the P^0 layer, μ_n and μ_p the mobility of electrons and holes respectively, and τ the lifetime of the injected electrons. As previously defined, L is the width of the P^0 layer. The Ashley-Milnes theory represents a recombination-limited solution of the continuity of equations for the electron and hole currents.

- *Onset of negative resistance characteristics with and without external illumination*

For the structure described above one would expect, on the basis of the theory proposed by Lampert,[5] a negative resistance regime in the current-voltage relation when a certain threshold voltage is exceeded. For the diodes studied by Weiser and Levitt,[6] however, it was concluded that the negative resistance observed was not caused by Lampert's mechanism since it set in at far lower voltages than would be predicted by that theory. On the other hand, a completely different mechanism suggested by Dumke was found to predict the phenomenon at voltages comparable to those actually observed. We shall therefore deal with the latter theory only.

In Dumke's theory the negative resistance is brought about in the following manner: The electrons which traverse the high resistance region combine with holes near the P-P^0 boundary. This recombination will at least be partly radiative, and the light emitted can be reabsorbed in the P^0 region, creating electron-hole pairs. Because of the presence of the negatively charged centers which are presumed to have a very large capture cross section for holes, the latter are immobilized, and hence do not contribute to the conduction process. The electrons, however, are driven across to the P-P^0 boundary, recombine in part radiatively, and hence create more electron-hole pairs. The process can, of course, be regenerative only if the quantum efficiency is high enough and the field is strong enough so that new electrons can be created in the P^0 region at a faster rate than that at which they decay. A further point to be made is that this process will lead to a negative resistance as opposed to a simple feed-back process, only if the quantum efficiency is an increasing function of the current at the beginning of the process. Under these conditions, the regenerative process can be sustained at lower and lower voltages as the quantum efficiency increases. The process stops, and hence the dynamic resistance becomes positive again, when the quantum efficiency reaches a constant value.

The formulation of the theory starts with the rate equation for the production of electron-hole pairs in the P^0 layer. The rate at which excess electrons, Δn, are produced is given by:

$$d\Delta n/dt = \frac{\phi\gamma(j)}{Le} j - \frac{\Delta n}{\tau}, \tag{2}$$

where ϕ is the fraction of photons which is absorbed in the P^0 region, and $\gamma(j)$ is the quantum efficiency at the P-P^0 boundary. Eq. 2 implies uniform absorption and therefore uniform creation of electron-hole pairs. This approximation is easily satisfied in GaAs diodes as will be discussed below.

If, at time zero, the current is the electron current given by Eq. (1b), the presence of the extra electrons produced by the light will add an ohmic component to the current because of the charge neutralization by the extra, immobile holes. The total current density will then be given by:

$$j = aV^2 + \Delta ne\mu_n V/L. \tag{3}$$

Substituting Eq. (3) into Eq. (2), yields

$$d\Delta n/dt = \frac{\phi\gamma(j)}{Le}\left(aV^2 + \Delta ne\mu_n \frac{V}{L}\right) - \frac{\Delta n}{\tau}. \tag{4}$$

We shall first consider the case of constant quantum efficiency, which reduces Eq. (4) to the form $d\Delta n/dt = R + k\Delta n$, where $R = (\phi\gamma aV^2)/(Le)$ and $k = (\phi\gamma\mu V)/(L^2) - (1/\tau)$. It is well known that the solution to Eq. (4) for this case is such that Δn will go to infinity as $t \to \infty$ if $k > 0$, but that Δn will reach a steady state value as $t \to \infty$ if $k < 0$. A critical voltage, V_s, will then correspond to $k = 0$, and will be given by:

$$V_s = (L^2)/(\phi\gamma\mu\tau). \tag{5}$$

For voltages higher than V_s a regenerative process will set in.

We shall now consider the more general case of letting the quantum efficiency be a function of current. A simple form of the dependence of γ on j, suggested by Dumke,[8b] is given by:

$$\gamma = \gamma_\infty(j^m)/(j^m + b). \tag{6}$$

Substituting Eq. (6) into Eq. (2) yields:

$$\frac{d\Delta n}{dt} = \frac{\phi\gamma_\infty}{Le}\frac{j^{m+1}}{(j^m + b)} - \frac{\Delta n}{\tau}. \tag{7}$$

We now simplify Eq. (7) by setting $m = 1$* and by assuming that at the onset of the negative resistance the quantum efficiency still depends strongly on the current so that Eq. (6) is adequately approximated by $\gamma \sim \gamma_\infty j/b$. Making use of Eq. (3) for the current we then write:

$$d\frac{\Delta n}{dt} = \frac{\phi\gamma_\infty}{Leb}\left(aV^2 + \Delta ne\mu_n\frac{V}{L}\right)^2 - \frac{\Delta n}{\tau} \tag{8a}$$

$$= u\Delta n^2 + v\Delta n + w, \tag{8b}$$

where

$$u \equiv \frac{\phi\gamma_\infty e\mu_n^2 V^2}{bL^3}, \qquad v \equiv \frac{2\phi\gamma_\infty a\mu_n V^3}{bL^2} - \frac{1}{\tau},$$

and

$$w \equiv \frac{\phi\gamma_\infty a^2 V^4}{Leb}.$$

Eq. (8) has two types of solutions depending on whether $q \equiv (4uw - v^2)$ is greater or smaller than zero. As shown below, the solution for $q < 0$ does not lead to any drastic increase in current with time while the solution for $q > 0$ leads to a regenerative process which produces a negative resistance in the presence of an external series resistance. A threshold voltage $V_{\rm th}$ can then be derived from the condition $q = 0$:

$$V_{th} = (bL^2/4\phi\gamma_\infty a\mu_n\tau)^{1/3}. \tag{9a}$$

It is instructive to express the factor a in the denominator in terms of parameters of the P^0 region, as given by Eq. (1b):

$$V_{th} = (bL^5/4e\mu_n^2\mu_p p_0\tau^2\phi\gamma_\infty)^{1/3}. \tag{9b}$$

Eq. (9b) expresses the threshold voltage in terms of measurable or calculable parameters. As the threshold voltage is exceeded the generation rate of excess carriers will be greater than their decay rate, and hence the current will rise with time. Since, however, by Eq. (6) a rise in current will lead to an increasing quantum efficiency, the voltage necessary to maintain the critical generation rate can be reduced. A negative resistance regime will set in, and will continue until the quantum efficiency becomes constant, and the voltage given by Eq. 5 is reached. Again making use of Eq. (1b), we find that the two voltages between which the resistance is negative are related by:

$$V_{\rm th}/V_s = b/4j_{\rm th}. \tag{10}$$

Since the negative resistance is brought about by the generation of electrons in the P^0 region by light given off at the P-P^0 boundary one may expect that external illumination would tend to lower the threshold voltage. Again making the approximation that the light is uniformly absorbed in the P^0 layer, we write Eq. (8a) to take into account the presence of external illumination of intensity I. Thus,

$$d\frac{\Delta n}{dt} = \frac{\phi\gamma_\infty}{Leb}\left(aV^2 + \Delta ne\mu_n\frac{V}{L}\right)^2 + \alpha I - \frac{\Delta n}{\tau} \tag{11a}$$

$$= u\Delta n^2 + v\Delta n + w + \alpha I. \tag{11b}$$

In this equation I is given in photons/cm^2/sec, and α is the absorption constant of the light; the symbols u, v, and w have the same significance as in Eq. (8b). We now solve for the critical value of voltage or light intensity beyond which Δn will go to infinity with time. This condition is obtained again by setting $q = 4uw' - v^2$ equal to 0, where $w' \equiv w + \alpha I$. We find that the critical light intensity $I_{\rm th}$ is given by:

$$I_{\rm th} = \frac{bL^3}{4\phi e\mu_n^2\alpha\tau^2 V^2}\left(1 - \frac{4\phi\mu_n\tau a V^3}{bL^2}\right). \tag{12a}$$

Making use of Eqs. (1b) and (9), we obtain

$$I_{\rm th} = \frac{V_{\rm th}j_{\rm th}L}{e\mu\alpha\tau(V_{\rm th}^I)^2}\left[1 - \left(\frac{V_{\rm th}^I}{V_{\rm th}}\right)^3\right]. \tag{12b}$$

This expression relates $V_{\rm th}^I$, the breakdown voltage in the presence of external illumination, to the incident light intensity. We see that $V_{\rm th}^I$ is proportional to $I^{-\frac{1}{2}}$, in the case of practical interest where the light intensity is high enough so that the breakdown voltage is reduced considerably. It is also interesting to note that the light sensitivity is proportional to the lifetime τ. Since, as discussed below, the switching speed of these diodes is inversely proportional to τ, light sensitivity and speed bear an inverse relation to each other.

• *Response of diodes to square voltage or light pulses*

(a) Pulses insufficient to cause breakdown

We now consider the behavior of these diodes upon application of a square voltage pulse, or upon exposure to a square light pulse, either of which has a value of zero at time 0. In the absence of external illumination the rate of increase of electrons in the P^0 layer is given by Eq. (8). For voltages below the critical voltage, so that $q < 0$, the solution to Eq. (8b) is given by

* We are indebted to R. W. Keyes for pointing out that this simplification greatly facilitates the solution of Eq. (8).

$$t = \frac{1}{\sqrt{-q}}\left[\log\frac{2u\Delta n + v - \sqrt{-q}}{2u\Delta n + v + \sqrt{-q}} - \log\frac{v - \sqrt{-q}}{v + \sqrt{-q}}\right]. \qquad (13)$$

The symbols u, v, and q have been defined in connection with Eq. (8b). For a value of Δn equal to $(\sqrt{-q} - v)/2u$, t approaches infinity; hence, a steady state value Δn_f will be given by this condition, and a current equal to $(aV^2 + \Delta n_f e\mu_n V/L)$ will flow through the diode. For an applied voltage such that $(V/V_{\text{th}})^3 \ll 1$, it is easily shown that the additional electron concentration Δn_f equals $w\tau$, and that this steady state value is reached approximately within a time τ. In the case of external illumination, the additional electron concentration for $(V/V_{\text{th}})^3 \ll 1$ becomes equal to $(w + \alpha I)\tau$.

(b) Pulses sufficient to cause breakdown

If the voltage pulse, applied from a constant voltage source, exceeds the critical value given by Eqs. (9) the current will increase drastically with time. Since in any circuit there will be a resistance in series with the diode, this increase in current will lead to a voltage drop across the diode. As discussed above, the voltage drop can be tolerated without a decrease in current because of the increase in quantum efficiency with increasing current; the negative resistance regime will cease when quantum efficiency becomes constant and V_s (Eq. 5) is reached. We wish to estimate the total switching time, i.e., the time needed to reach V_s. Before the voltage across the diode changes appreciably the current has to build up to the point where the change in voltage across the series resistance is an appreciable fraction of the initial voltage across the diode. This "delay" period admits solution by Eqs. (8) under essentially constant voltage conditions. To estimate this delay time we shall take as an example the case of an external series resistance such that it requires a doubling of the initial current, aV^2, (see Eq. (1b)), to bring about an appreciable voltage change. For $V > V_{\text{th}}$, i.e. $q > 0$, the solution of Eq. (8b) is:

$$t_d = \frac{2}{\sqrt{q}}\left[\tan^{-1}\frac{2u\Delta n + v}{\sqrt{q}}\right]_{\Delta n=0}^{\Delta n_d}, \qquad (14a)$$

where Δn_d is the excess electron density at the end of the delay period t_d. Substituting for u, v, and w (recognizing that external illumination is absent), and making use of Eqs. (9), we find that

$$t_d = \frac{2\tau}{\left[\left(\frac{V}{V_{th}}\right)^3 - 1\right]^{1/2}}\left\{\tan^{-1}\frac{\frac{V}{2aV_{th}^3}\left(e\mu_n\Delta n\frac{V}{L} + aV^2\right) - 1}{\left[\left(\frac{V}{V_{th}}\right)^3 - 1\right]^{1/2}}\right\}_{\Delta n=0}^{\Delta n_d} \qquad (14b)$$

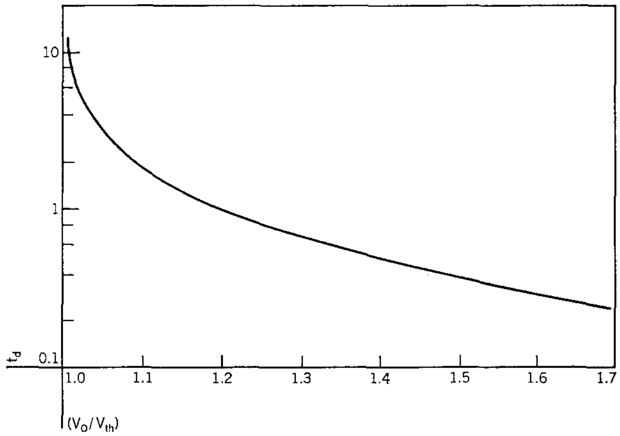

Figure 2 Delay time t_d calculated from Eq. (14c) with $2\tau = 1$.

As stated above, we shall assume that the end of the "delay" period is given by the condition that the photocurrent equals the initial current. Hence, setting Δn_d equal to $aLV_0/e\mu$, we find the following expression for the delay time t_d:

$$t_d = \frac{2\tau}{\left[\left(\frac{V}{V_{\text{th}}}\right)^3 - 1\right]^{1/2}}\left\{\tan^{-1}\frac{\left(\frac{V}{V_{\text{th}}}\right)^3 - 1}{\left[\left(\frac{V}{V_{\text{th}}}\right)^3 - 1\right]^{1/2}} - \tan^{-1}\frac{\frac{1}{2}\left(\frac{V}{V_{\text{th}}}\right)^3 - 1}{\left[\left(\frac{V}{V_{\text{th}}}\right)^3 - 1\right]^{1/2}}\right\} \qquad (14c)$$

In Figure 2 we plot the delay time as given by Eq. (14c) as a function of V_0/V_{th}. For considerable overdrive, i.e., $(V_0/V_{\text{th}})^3 \gg 1$, the arctan can be expanded in series form, and Eq. (14c) acquires the simple form

$$t_d \sim 2\tau(V_{\text{th}}/V)^3. \qquad (14d)$$

It is worth noting that if the series resistance is small enough so that the photocurrent can build up to many times the value of the initial current, aV^2, before an appreciable voltage drop sets in, the above expression is increased only by a factor of about two.

Equations (14a-d) are solutions of Eq. (8a), which was derived from Eq. (7) by making the simplifying assumption that the quantum efficiency depends linearly on current. Since a superlinear dependence, i.e., $m > 1$ in Eq. (7), would lead to a more rapid increase of the electron concentration with time, it is clear that Eqs. (14a–d) represent an upper limit for the delay period. As will be discussed in the experimental section, even longer delay times than those predicted by these equations have been found experimentally. Hence, to expend much greater labor to solve Eq. (7) without the simplifying assumptions we have employed seems hardly justifiable.

In the presence of external illumination, the rate of generation of electrons is given by Eq. (11b) which is of the same form as Eq. (8b). For a light intensity greater than the critical value I_{th} given by Eq. (12), the delay time for switching by means of a light pulse will be given by:

$$t_d = 2\tau I_{th}/I, \quad \text{for} \quad I/I_{th} \gg 1. \tag{15}$$

Once the photoconductive current has increased to the point where the voltage across the external series resistance has changed appreciably, the voltage across the P^0 region is no longer the initial voltage V_0 but rather $V_0/(1 + \Delta ne\mu AR/L)$, where A is the cross sectional area of the diode and R is the load resistance. We have assumed that the inductive and capacitative reactances of the circuit are negligible. Equations (8) still apply, of course, but with V which is a function of n, and hence of the current. The equation cannot be solved analytically under these circumstances, and we shall derive the solution for the simpler case of constant quantum efficiency. We shall also ignore the term aV^2 in Eq. (8a) which is tantamount to assuming that at the end of the delay period, the photoconductive current is considerably larger than the original current given by aV^2. With these approximations the switching time calculated will be an upper limit since we ignore the fact that the switching occurs more rapidly at the beginning while the quantum efficiency is still changing, and also ignore the aV^2 component of the current which aids the production of the photocurrent. The rate of change of electrons for this case is then given by:

$$d\frac{\Delta n}{dt} = \frac{\phi\gamma}{L^2}\mu_n V_0\left(\frac{\Delta n}{1 + e\mu n AR\Delta n/L}\right) - \frac{\Delta n}{\tau}, \tag{16a}$$

$$= h\frac{\Delta n}{1 + g\Delta n} - \frac{\Delta n}{\tau}, \tag{16b}$$

where $h \equiv \phi\gamma\mu_n V_0/L^2$ and $g \equiv e\mu AR/L$. The solution for the switching time t_s is given by:

$$t_s = -\frac{\tau}{h\tau - 1}\log\left[\frac{h\tau - 1 - gn}{gn}\right]_{\Delta n_d}^{\Delta n_f} - \tau\log\left[h\tau - 1 - gn\right]_{\Delta n_d}^{\Delta n_f} \tag{17a}$$

The upper limit, Δn_f, will be given by the condition $[V_0/1 + \Delta n_f e\mu AR/L] = V_s$, where V_s is given by Eq. (5). The lower limit, Δn_d, is approximately given by $i_0 L/Ae\mu_n V_0$, where i_0 is the current which flows upon application of the voltage pulse. The upper limit Δn_f is reached at $t = \infty$. For the practical conditions that $V_0/V_s \gg 1$, and $i_0 R \ll V_0$, 90% of the final current is reached in a time:*

$$t_s \sim \tau\frac{V_s}{V_0}\log\frac{V_0/V_s}{i_0 R/V_0}. \tag{17b}$$

We see that in the absence of inductance the switching time can easily be made a small fraction of the lifetime τ.

Experimental results

• *Method of fabrication and summary of properties*

Diodes with a P-P^0-N structure were fabricated by two different techniques: In the original experiments[6] n-type GaAs ($n \sim 3 \times 10^{17}$ cm^{-3}) provided the starting material, and manganese was then diffused into it at 900°C until a P^0-N junction depth of typically 100μ was reached. A much shallower zinc diffusion providing a low resistivity layer on top of the P^0 region was then carried out. Two types of manganese diffusion techniques were employed, namely, with and without excess arsenic in the vial. In the former case (Method I, Table 1) the arsenic pressure

Table 1 Characteristics of diodes with P-P^0-N structure produced by different techniques.

Method of fabrication	*Temperature range of negative resistance*	*Total typical switching speeds*[b]	*Light sensitivity*[c]
I: Double diffusion; no excess arsenic pressure[a]	100°K	3×10^{-6} sec (77°K)	Fair
II: Double diffusion; excess arsenic pressure	Often up to 300°K	6×10^{-7} sec (77°K)	High
III: Vapor deposition plus diffusion	Up to 300°K	4×10^{-9} sec (300°K)	Poor

[a] The diodes produced by this technique were those discussed in Ref. 6.
[b] As discussed in the section on theory, the total switching speed (delay time plus switching time) will depend on over-voltage. The speeds given in column 3, above, are typical for $V/V_{th} = 2$.
[c] The three classifications of high, fair, and poor light sensitivity are based on the magnitude of voltage below V_{th} which could be tolerated and still permit switching by a microscope light at a distance of a few centimeters away. In the case of high light-sensitivity, switching could be accomplished at several volts below V_{th}; at the other extreme of poor light sensitivity, a bias only about 0.1 V below V_{th} could be tolerated.

* A similar expression for the switching time, using somewhat different approximations has been derived from Dumke (unpublished).

was approximately 10^{-3} atmospheres; in the latter case, (Method II, Table 1) the arsenic pressures were typically several atmospheres. In a very different technique[10] for achieving this structure (Method III, Table 1), a slice of manganese-doped GaAs was employed as the starting material and an n-layer ($n \sim 1 \times 10^{18}$ cm^{-3}) was deposited on one side of it by vapor deposition; zinc was then diffused into the other side to provide the low resistivity p-layer. The P-P^0 boundary and the P^0-N junction could be determined by electrolytic etching. In all these techniques the width of the P^0 region could be controlled by the depth of the zinc diffusion. Widths of the P^0 region from 2 to 40 μ were investigated. The last mentioned structure, in addition to providing the negative resistance described below, yielded lasers in which high order transverse modes were clearly observed.[1b] Diodes produced by Method II also produced lasers[11] though not reproducibly. The chief characteristics of the diodes produced by these three techniques are listed in Table 1 and a schematic diagram of a typical unit is provided in Fig. 3.

In general, the reproducibility of properties of diodes produced by Method I and III was high while that of diodes produced by Method II was poor. In addition, diodes produced by Method II showed pronounced trapping effects, not shown by diodes produced by the other two techniques. The trapping effects showed up in pulsed operation, in that the breakdown voltage for pulses beyond the first pulse was found to be a function of the repetition rate. Thus the advantage of high light sensitivity was gained at the expense of trapping effects and general lack of reproducibility. As a result, studies of these diodes, some of which produced lasers, were confined to switching experiments by light.[11] By contrast, diodes produced by Methods I and III were studied extensively both with respect to electrical and electroluminescent properties.

Figure 3 Typical dimensions of P-P^0-N diodes (drawn approximately to scale).

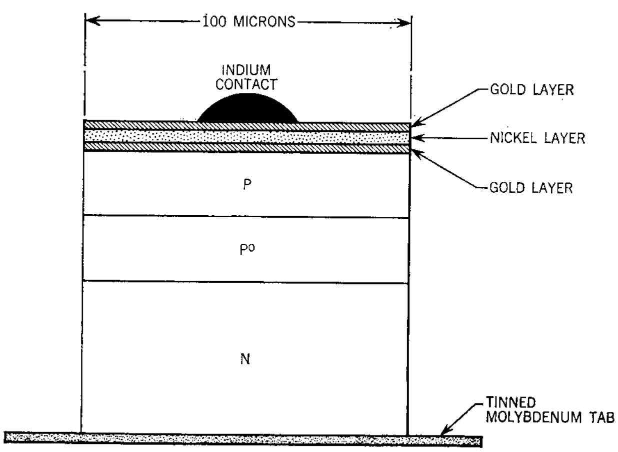

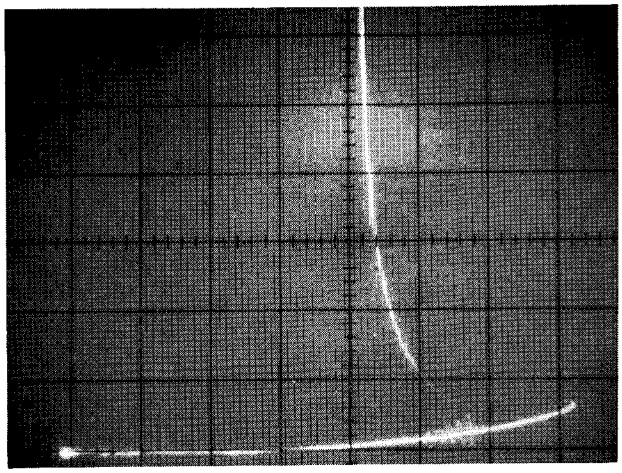

(*a*)

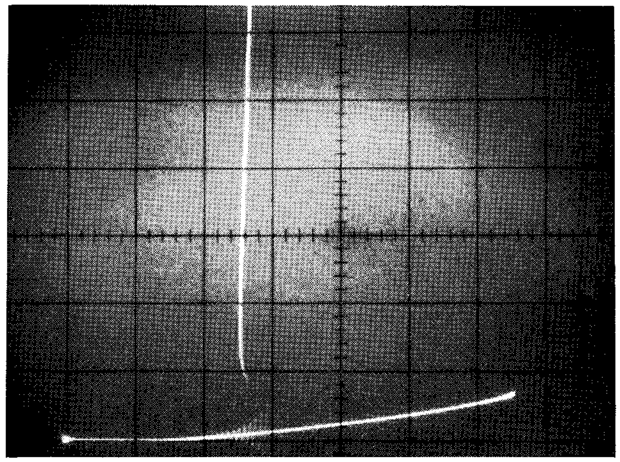

(*b*)

Figure 4 Typical Current-Voltage Characteristics of P-P^0-N diodes. Diode A was produced by Method I of Table 1; characteristics were taken at 77°K. Here $L = 4 \times 10^{-3}$ cm, $A = 5 \times 10^{-4}$ cm^2. Diode B was produced by Method III of Table 1; characteristics were taken at 300°K. Here $L = 9 \times 10^{-4}$, $A = 3 \times 10^{-4}$ cm^2. For diode A the vertical scale is 2 mA/div; the horizontal, 0.5 V/div. For diode B the vertical scale is 10 mA/div; the horizontal, 0.5 V/div.

• *Comparison of static characteristics with theory*

In Fig. 4 we show quasi-dc current-voltage characteristics for two diodes produced by Methods I and III of Table 1, diodes A and B, respectively. The voltage was applied from a high-impedance, half-wave-rectified, 60-cps voltage source. The characteristics of diode A were taken at 77°K, while those of diode B were taken at room temperature. It is surprising at first glance that the breakdown voltages for both of these diodes—prepared by such different techniques and taken at different temperatures—should be approximately the same.

In comparing these results one may start out by examining whether the current-voltage relations in the pre-breakdown regime of the two diodes follow the Ashley-Milnes theory.[7] In particular, in order for Dumke's theory[8] to apply to both diodes, one would have to see whether, just before breakdown, most of the current is carried by electrons across the P^0 region. In Fig. 5 we plot the current-voltage relation for the same two diodes, and we find that the Ashley-Milnes theory (Eq. (1a) and (1b)) is indeed obeyed.* For diode A it was actually ascertained[6] that for currents near breakdown most of the light originates at the P-P^0 boundary as expected when the square law is followed. The effect is not noticeable in the case of diode B at room temperature though it is at 77°K.[1b] The reason probably is that the voltage range before breakdown over which the current is carried essentially by electrons, is very small, as seen from Fig. 5. It is interesting that the lifetimes ($\tau = L^2/\mu_n V_\tau$) computed from the voltage V_τ where the linear and the square law regimes of Fig. 5 intersect[7] are very different for the two diodes. The lifetime estimated for diode A is about 10^{-8} sec while that for diode B is of the order of 10^{-10} sec. These estimates are very approximate by virtue of the uncertainty in the appropriate values for the electron mobility, which was taken as 4000 cm^2/V sec. Examination of the spectral distribution of the light emitted before breakdown sheds light on the difference between these two lifetimes. For diodes of type A, it was shown[6] that recombination at 77°K occurs through the manganese centers, at an energy of about 0.1 eV lower than the gap energy. The lifetime of 10^{-8} sec estimated for Fig. 5 for such diodes is in good agreement with that calculated theoretically[12] for such a recombination. A similar examination at room temperature of the light emission from diodes of type B shows, on the other hand, that light emission occurs at an energy within 0.01 eV of the bandgap, and hence a much shorter lifetime is to be expected.[12] During the pre-negative resistance regime, the quantum efficiency is not constant but increases rapidly with current for both types of diodes, as had been previously reported for diodes of type A.[6b]

We can now insert the parameters calculable from Fig. 5 into Eq. (9b) to predict the breakdown voltages for diodes A and B of that Figure. Substituting $L^2/\mu_n V_t$ for τ, it is possible to reduce Eq. (9b) to the form $V_{th} = (bV_t^2 R_\Omega A/4\phi\gamma_\infty)^{\frac{1}{3}}$, where R_Ω is the ohmic resistance of the P^0 region. The value of b can be obtained from light intensity vs current, and V_t and R_Ω can be obtained from the curves of Fig. 5. Assuming $\phi \sim 0.3$, and $\gamma_\infty \sim 0.5$, and knowing the area of the diode, we calculate a value of V_{th} equal to 2.9 V for diode A. To compare this value

* While diode B of Fig. 5 obeyed the Ashley-Milnes theory at room temperature a more complicated behavior was followed at 77°K. In general, diodes of type A obeyed the Ashley-Milnes theory while diodes of type B sometimes exhibited more complicated behavior.

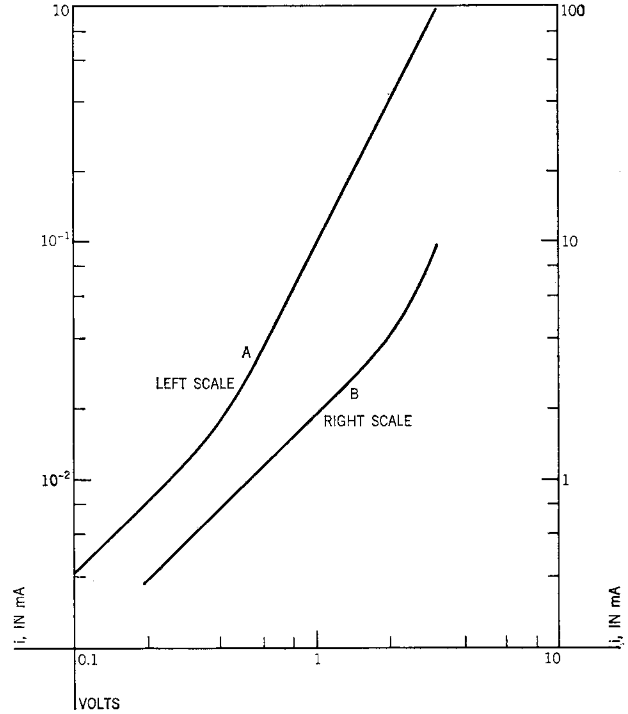

Figure 5 Current vs voltage in P^0 region. Diode A (Method I of Table 1) data taken at 77°K; diode B (Method III of Table 1) data taken at 300°K. The voltage across the P^0 region was estimated by subtracting the junction voltage from the total voltage; see Ref. 6.

to the experimental threshold voltage of 3.7 V as shown in Fig. 4, we must add the junction voltage of 1.4 V to the theoretical value of 2.9 V, thus arriving at a value 4.3 V. The agreement between the theoretical and the experimental values is clearly excellent. In view of the uncertainty with regard to the exact values of ϕ and γ_∞, such close agreement may be somewhat fortuitous but since the estimate for these parameters is probably correct as to order of magnitude, the agreement between theory and experiment is very satisfactory for any reasonable values of ϕ and γ_∞. Performing a similar estimate for diode B of Fig. 5, we arrive at a value of 10 V for V_{th}, using the same values for ϕ and γ_∞ as for diode A. Since the quantum efficiency at room temperature is usually less than at liquid nitrogen temperature, a more realistic value for γ_∞ would raise the calculated value of V_{th} somewhat. The estimates are in reasonable agreement with the experimental value of 3.3 V for diode B shown in Fig. 4, though the agreement is not as good as for diode A.

We shall now turn to an examination of the light sensitivity of diodes to check the validity of Eqs. (12). A quantitative study was undertaken only for the case of a diode produced by Method I of Table 1. In Fig. 4 we show the current-voltage characteristics of diode 116B5 under ex-

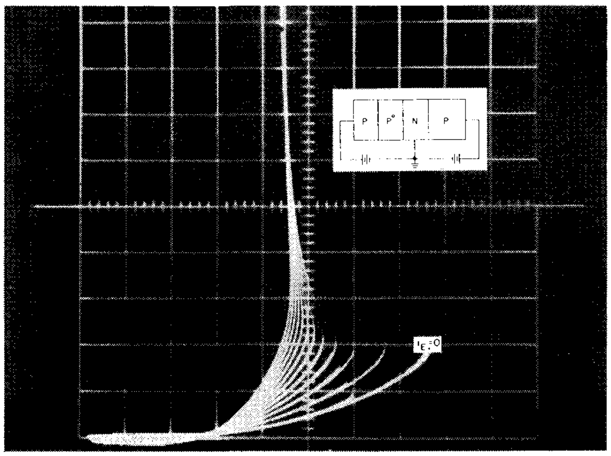

Figure 6 Effect of external illumination. Current-voltage characteristics (77°K) for diode produced by Method I of Table 1, as function of current i_E through *P-N* junction of four layer structure shown in insert. Proceeding from outermost curve, corresponding to $i_E = 0$, each successive curve represents an increase of 2 mA in current through the *P-N* junction. Scales: 0.5 V per horizontal division, 1 mA per vertical division.

ternal illumination, as reported by Levitt et al.[14] The experiment was performed with the aid of a four-layer structure shown schematically in the insert in Fig. 6. The illumination of the P^0 region was accomplished by the light given off at the *P-N* junction when current was passed across it in the forward direction. It was ascertained that the quantum efficiency for this process was constant. A study of the breakdown voltages as a function of the current i_E through the *P-N* junction thus permits an examination of the validity of Eqs. (12). If we further assume 100% quantum efficiency for this current, and neglect the very small absorption of the light in the *n*-region,[13] the magnitude of the parameters in Eqs. (12) can be examined. We first note, however, that the basic assumption of Eq. (3), namely, that the photoconductive current is simply additive to the current in the absence of light seems to be borne out. In Fig. 7 we plot the photocurrent Δi at one volt across the P^0 region, against the current i_E across the *P-N* junction. The value of Δi is obtained by subtracting from the total current at a given i_E the current for $i_E = 0$; the voltage across the P^0 region is obtained by subtracting from the total voltage a junction voltage of 1.4 V, as discussed in Reference 6. We see that Δi is proportional to i_E at this voltage; a linear relation was also found at other voltages sufficiently below V_{th}. Since $\Delta i = A\Delta n e\mu_n V/L$, and $\Delta n = i_E\alpha\tau/2Ae$, the slope of Fig. 7 equals $\alpha\tau\mu_n V/2L$. (The factor of 2 appears in these relations because we assume that one half of the light emitted at the *P-N* junction travels in the direction to the P^0 region). Using the value of 10^{-8} sec for τ as estimated from Fig. 5 and taking $\mu_n = 4000$ cm^2/V sec, and $L = 4 \times 10^{-3}$ cm,[6] we obtain a lower limit of 50 cm^{-1} for the absorption constant α, which is quite reasonable for compensated manganese-doped GaAs.[15] Substituting $i/2Ae$ for I_{th} in Eq. (12b) and using the value for $\alpha\tau$ as determined from the slope of Fig. 7 permits us to construct a theoretical curve for the breakdown voltage as a function of i_E. This curve together with the experimental points is plotted in Fig. 8. The agreement between theory and experiment is clearly excellent.

- *Transient behavior under excess voltage or light pulses*

The analysis of diode response in the earlier section on theory suggests that the total switching speed, (i.e., the

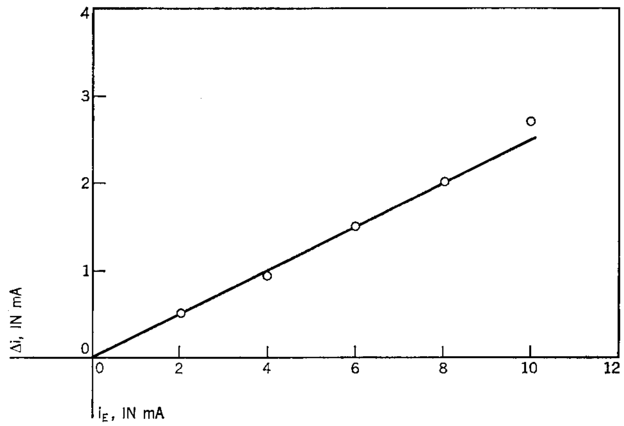

Figure 7 Photocurrent, Δi, at 1V across the P^0 region as a function of current i_E through the *P-N* junction in four-layer structure shown in the insert of Fig. 6.

Figure 8 Threshold voltage under external illumination (V_{th}^I) as a function of current i_E through *P-N* junction in four-layer structure shown in Fig. 6. Solid line is theoretical curve based on Eq. (12b) using value of $\alpha\ \tau$ derived from Fig. 7.

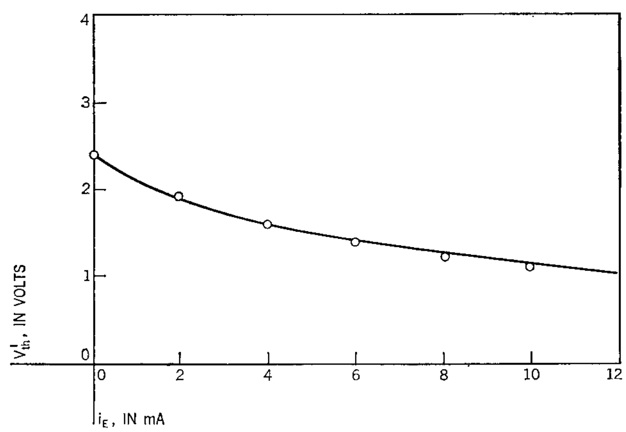

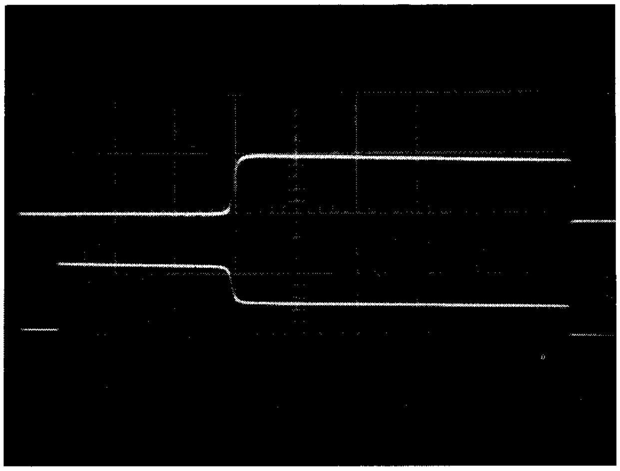

(a)

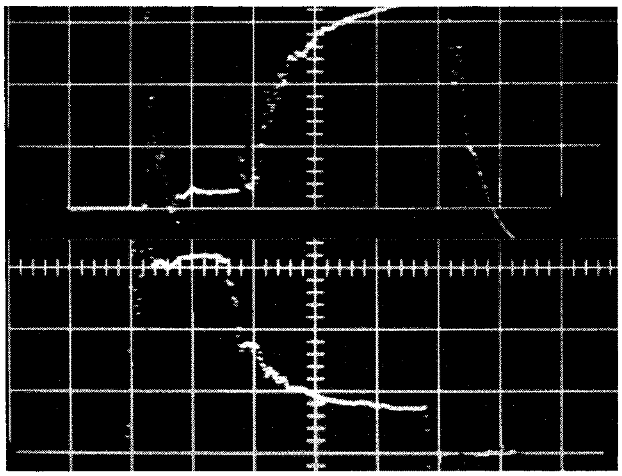

(b)

Figure 9 Voltage vs time (lower trace) and current vs time (upper trace) for a voltage pulse in excess of breakdown voltage. Photograph (a) was taken at 77°K for Diode A of Fig. 2; photograph (b) was taken at 300°K for Diode B of Fig. 2.

Scales are as follows: For diode A—horizontal, 5 μsec/div; vertical (upper trace), 100 mA/div; vertical (lower trace), 5 V/div. For diode B—horizontal, 10 nsec/div; vertical (upper trace), 40 mA/div; vertical (lower trace), 1 V/div.

time needed for the diodes to change from a high-voltage, high-resistance state to a low-voltage, low-resistance state) can be divided into a delay time and a switching time, and that both of these should decrease with increasing excess voltage. It was pointed out that in the absence of inductive effects, the delay time will depend on the magnitude of the external resistance. As an example, we shall discuss the situation actually employed in these experiments, in which a constant voltage generator was used in series with the diode and a resistor of 100 ohms. Suppose that a diode has a breakdown voltage of 3 V, at which point it draws 3 mA of current. If a 5 V pulse is applied to the diode, then, from Eq. (1b) about 5 mA will flow through it initially. (For the sake of simplicity we ignore the voltage across the junction). If we call the end of the delay time the time needed for the voltage to decrease by 10%, it is clear that for a resistance of 100 ohm the current will have to increase by 5 mA to give rise to the stipulated voltage change of 10%. Eq. (14c), which gives the time needed for the current to double at constant voltage, thus applies fairly well to the situation actually studied.

Figure 9 shows the behavior of voltage vs time, and current vs time, for the two diodes whose d-c characteristics are shown in Fig. 4, when a voltage pulse in excess of the threshold voltage is applied. As before, diode A was studied at 77°K while diode B was studied at room temperature. It is obvious that there is indeed a delay time before the onset of switching, and that the delay is much greater for diode A than for diode B. These diodes are respectively typical of those prepared by Methods I and III of Table 1. In Fig. 10 we show, using diode B as an example, how the delay time decreases with increasing overvoltage, as had previously been reported for diodes of type A.[6] With overvoltages of the order of 2 or 3 volts most diodes of type B were found to have delay times of less than 4 nsec, and switching times of 1 to 2 nsec. Since the lifetime in the P^0 region can be estimated from plots like that shown in Fig. 5 by means of the Ashley-Milnes theory,[7] one should be able to predict the delay time for a given value of V/V_{th} from Eq. (14c). The lifetimes for diodes A and B in Fig. 5 were estimated to be 1×10^{-8}

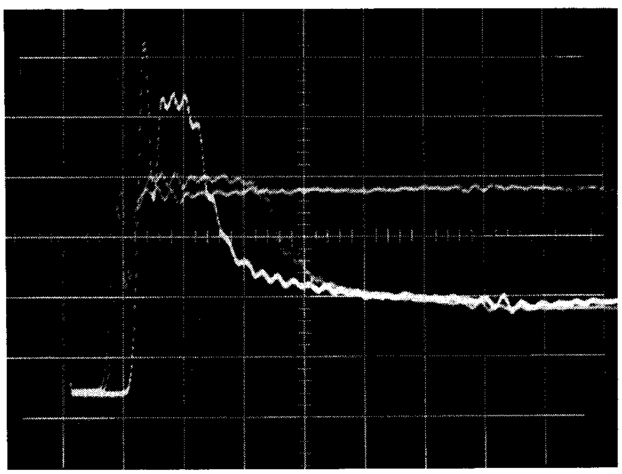

Figure 10 Decrease of delay time as function of overvoltage. Diode fabricated by Method III of Table 1; data taken at 300°K. Scale: 1 V/vertical division, 5 nsec/horizontal division.

sec and 2×10^{-10} sec respectively. For the voltage pulses shown in Fig. 9, V/V_{th} is approximately 2 for diode A, approximately 1.06 for diode B. The calculated delay time from Eq. (14c) should thus be approximately 2×10^{-9} sec for either diode. Experimentally, the delay time for diode A is about 1000 times longer than that predicted from the theory, while the delay time for diode B is about 6 times longer than its theoretical value. Similarly, the switching times of about 10^{-6} sec for diode A and 2×10^{-9} sec for diode B are much longer than would be expected on the basis of Eq. (17b). In all cases studied, the total switching speeds were orders of magnitude longer than predicted by the theory for diodes produced by Methods I or II of Table 1, and about ten times longer for diodes of Method III.

Only a brief investigation of the switching speed as a function of light intensity was made using a diode made by Method II of Table 1. It was found that the delay varied inversely with light intensity as predicted by Eq. (15). A GaAs laser pointing at the negative resistance diode served as the light source in these experiments.[11]

Conclusions

From data for double-diffused diodes presented in earlier publications and from the data for diodes with a uniformly doped central region presented in this paper, it appears that the static negative resistance behavior of the diodes is in good agreement with Dumke's model. The main points of agreement can be summarized is follows: (1) For voltages below the onset of the negative resistance the transit time of electrons is less than their lifetime; thus they can traverse the P^0 region to recombine at the P-P^0 boundary. This behavior was confirmed by direct observation of the spatial origin of the radiative recombination in the case of the double-diffused diodes. (2) The radiative component of the recombination process is an increasing function of the current before the onset of the negative resistance. When the dynamic resistance becomes positive again, the quantum efficiency becomes constant. (3) The dynamic resistance of the P^0 region in the post-negative resistance regime is essentially zero. (4) The threshold voltage decreases with external illumination. (5) The theory is able to predict threshold and sustaining voltages as well as the effect of external illumination in a semiquantitative manner. The parameters which enter the theory can be obtained from a determination of the current-voltage relation before the onset of the negative resistance and from a determination of the dependence of the quantum efficiency on current. A more detailed investigation into the agreement of theory and static behavior would involve varying the width of the central region as well as the nature and concentration of the dominant impurity in it. The phenomenon should also be studied over a wider temperature range.

In this paper we have developed Dumke's model in a manner which enables us to predict the transient behavior of the diodes, i.e., their switching times upon application of a voltage pulse in excess of the threshold voltage. The theoretical expressions were derived under simplifying assumptions such that they represent upper limits for the switching times. In spite of this, the experimental switching times were found to be considerably longer than predicted by the theory. (It is encouraging in this respect that diodes prepared by a technique which provides a uniform central region have switching times of only a few nanoseconds at the moment). It is impossible to state the extent to which this disagreement sheds doubt on the validity of Dumke's model. In view of the impressive agreement of the theory with the static characteristics, one is inclined to believe the model, and to look for the source of the disagreement in factors that influence the transient behavior but not the static behavior. For example, one such factor may lie in a lack of homogeneity in the central region. If we consider layers perpendicular to the plane of the junction, it is possible that the breakdown conditions are first met in one of them—for example, in a surface layer. The breakdown can then spread to adjacent layers as a result of the increased light emission at the P-P^0 boundary and eventually engulf the whole P^0 region. Such a spreading process is probably much slower than a process in which the breakdown condition is reached simultaneously in all layers. It is also possible to construct models in which traps play a role in the switching characteristics but do not affect the static behavior. The existence of such traps was of course ignored in the theory as developed so far. Only further research with diodes in which the structure embodied in Fig. 1 is ever more closely approximated can hope to provide the experimental conditions against which the model can be tested rigorously.

Acknowledgments

We wish to acknowledge outstanding contributions by R. E. Fern to these investigations and, also, to thank F. R. Feigel and W. J. Fitzpatrick for their collaboration. We also thank J. M. Woodall for supplying us with manganese-doped GaAs, J. F. Wood for various Hall measurements, and H. Leonhardt and H. S. Rupprecht for depositing the N-layers. Finally, we express our gratitude to R. W. Keyes, M. I. Nathan and F. Stern for critical readings of the manuscript and for valuable discussions.

Note added in proof

In the section on the comparison of static characteristics with theory, the static characteristics of diodes produced by Method III were discussed, and it was found that good agreement with theory was obtained provided that curve B of Fig. 5 was interpreted in terms of the Ashley-Milnes theory. In other words, it was assumed that the departure from the linear current-voltage regime was due to the traversal of the P^0 region by electrons injected at the junction. Since this paper was written, it has been discovered that the diffusion of zinc into manganese-doped GaAs produces a thin, high-resistivity *p*-type layer at the boundary of the zinc layer (K. Weiser and J. F. Woods, to be published). It was ascertained that the resistivity of the bulk material remains unchanged as a result of the zinc diffusion.* As a result, the voltage drop across the P^0 region is concentrated near the boundary of the zinc region, and it can be shown that the voltage drop across the bulk of the P^0 region is insufficient to drive electrons across it unless an unreasonably long lifetime (approximately half a microsecond) is assumed for the injected electrons. It is therefore not permissible to interpret the curve B of Fig. 5 in the manner done in the paper since the voltage shown there is not actually dropped across the P^0 region as a whole. Nevertheless, it can easily be shown that the same basic mechanism which is treated in the paper probably gives rise to the negative resistance observed for diodes produced by Method III. It is only necessary to postulate that the first electrons created in the high-resistivity region are produced by absorbed light which originates at the P^0-N junction as a result of the radiative recombination of injected electrons. Once electrons are created in the high-resistivity region they are driven into the zinc layer by the electric field, where they recombine radiatively. The light can then again be absorbed in the high-resistivity region and create more electrons in it. As before, a critical voltage exists across the high-resistivity region, at which this process becomes regenerative so that a large increase in current results. Also, as before, a negative resistance will set in if the quantum efficiency increases with increasing current. While it is an easy matter to derive equations for the breakdown voltage and the sustaining voltage for this model, it is impossible at the moment to check these equations experimentally since the width of these high-resistivity regions is not known accurately.

* Such high-resistivity layers are not present in diodes produced by Method I.

References

1. (a) D. K. Wilson, *Symposium on Radiative Recombination in Semiconductors*, Dunod, Paris, 1964.
   (b) K. Weiser and F. Stern, *Appl. Phys. Letters* **5**, 115 (1964).
   (c) M. Pilkuhn and H. Rupprecht, *Bull. Amer. Phys. Soc., Ser II*, **10**, 96 (1965).
2. (a) N. Holonyak, Jr.; S. W. Ing, Jr.; R. C. Thomas; and S. F. Bevacqua, *Phys. Rev. Lett.* **8**, 426 (1962).
   (b) N. Holonyak, *Proc. IRE* **50**, 2421 (1962).
3. S. W. Ing, Jr., H. A. Jensen, and B. Stern, *Appl. Phys. Letters* **4**, 162 (1964).
4. T. Yamamoto, *Proc. IEEE* **52**, 409 (1964).
5. M. A. Lampert, *Phys. Rev.* **125**, 126 (1962).
6. K. Weiser and R. S. Levitt, *J. Appl. Phys.* **35**, 2431 (1964).
7. K. L. Ashley and A. G. Milnes, *J. Appl. Phys.* **35**, 369 (1964).
8. (a) W. P. Dumke, *Bull. Amer. Phys. Soc.* **9**, 217 (1964).
   (b) W. P. Dumke, *Proc. of 7th International Conference, Physics of Semiconductors*, Dunod, Paris (1964); p. 611.
9. See, for example, C. Hilsun and A. C. Rose-Innes, *Semiconducting III-V Compounds*, Pergamon Press, 1961, p. 139.
10. K. Weiser and R. W. Keyes—unpublished.
11. K. Weiser and A. E. Michel, *Symposium on Radiative Recombination in Semiconductors*, Dunod, Paris, 1964.
12. W. P. Dumke, private communication.
13. See, for example: W. J. Turner, W. E. Reese, and G. D. Pettit, *Phys. Rev.* **136**, A1467 (1964).
14. R. S. Levitt, K. Weiser, A. E. Michel and E. J. Walker, Solid State Device Conf. of IEEE, East Lansing, Michigan, June, 1963.
15. W. J. Turner and W. E. Reese—to be published.

Received April 20, 1965